11796 *Biochemistry* **2009,** *48,* 11796–11806
DOI: 10.1021/bi901571t

BIOCHEMISTRY
including biophysical chemistry & molecular biology
Article

Biophysical Analyses of Synthetic Amyloid-β(1−42) Aggregates before and after Covalent Cross-Linking. Implications for Deducing the Structure of Endogenous Amyloid-β Oligomers[†]

Brenda D. Moore, Vijayaraghavan Rangachari,[‡] William M. Tay, Nicole M. Milkovic, and Terrone L. Rosenberry*

Department of Neuroscience, Mayo Clinic College of Medicine, 4500 San Pablo Road, Jacksonville, Florida 32224. [‡]*Current address: Department of Chemistry and Biochemistry, 118 College Dr., University of Southern Mississippi, Hattiesburg, MS 39406-0001.*

Received September 8, 2009; Revised Manuscript Received November 3, 2009

ABSTRACT: A neuropathological hallmark of Alzheimer's disease (AD) is the presence of large numbers of senile plaques in the brain. These deposits are rich in fibrils that are composed of 40- and 42-residue amyloid-β (Aβ) peptides. Several lines of evidence indicate that soluble Aβ aggregates as well as fibrils are important in the etiology of AD. Low levels of endogenous soluble Aβ aggregates make them difficult to characterize, but several species in extracts of AD brains have been detected by gel electrophoresis in sodium dodecyl sulfate (SDS) and immunoblotting. Individual Aβ oligomers ranging in size from dimers through dodecamers of 4 kDa monomeric Aβ have been resolved in other laboratories as discrete species by size exclusion chromatography (SEC). In an effort to reconstitute soluble Aβ aggregates in vitro that resemble the endogenous soluble Aβ aggregates, we previously found that monomeric Aβ(1−42) rapidly forms soluble oligomers in the presence of dilute SDS micelles. Here we extend this work in two directions. First, we contrast the size and secondary structure of these oligomers with those of synthetic Aβ(1−42) fibrils. SEC and multiangle light scattering were used to obtain a molecular mass of 150 kDa for the isolated oligomers. The oligomers partially dissociated to monomers through nonamers when incubated with SDS, but in contrast to endogenous oligomers, we saw no evidence of these discrete species prior to SDS treatment. One hypothesis to explain this difference is that endogenous oligomers are stabilized by covalent cross-linking induced by unknown cellular agents. To explore this hypothesis, optimal mass spectrometry (MS) analysis procedures need to be developed for Aβ cross-linked in vitro. In our second series of studies, we began this process by treating monomeric and aggregated Aβ(1−42) with three cross-linking agents: transglutaminase, glutaraldehyde, and Cu(II) with peroxide. We compared the efficiency of covalent cross-linking with these agents, the effect of cross-linking on peptide secondary structure, the stability of the cross-linked structures to thermal unfolding, and the sites of peptide cross-linking obtained from proteolysis and MS.

Alzheimer's disease (AD)[1] is characterized by large numbers of senile plaques in the brain that are composed of fibrillar aggregates of 40- and 42-residue amyloid-β (Aβ) peptides. A number of investigators now propose that soluble aggregates of Aβ (protofibrils or oligomers), rather than monomers or insoluble amyloid fibrils, may be responsible for synaptic dysfunction in the brains of AD patients and AD animal models (*1*−*5*). This proposal is supported by observations that soluble aggregates generated in vitro from synthetic Aβ(1−40) and Aβ(1−42) induced toxicity in cultured cells (*2*, *6*), that soluble Aβ aggregates produced in cell cultures markedly inhibited hippocampal long-term potentiation in rats in vivo (*7*), and that transgenic mice expressing human Aβ showed functional deficits that precede extracellular deposition of fibrillar Aβ (*4*, *8*). These endogenous soluble Aβ aggregates are present in brain extracts from AD patients (*9*) and transgenic mice that express human Aβ (*10*), and several species have been detected by gel electrophoresis in sodium dodecyl sulfate (SDS) and isolated by size exclusion chromatography (SEC) (*10*, *11*). However, these aggregates are present at low levels, which make it difficult to characterize their structure.

A complementary strategy is to reconstitute soluble Aβ aggregates in vitro from synthetic Aβ which reproduce the biochemical and pathophysiological features of the endogenous soluble Aβ aggregates. However, simple incubation of Aβ peptides in aqueous buffers results primarily in mixtures of monomers, protofibrils, and fibrils with at most a minor amount of small oligomers (*12*−*14*). Aβ aggregation is stimulated at interfaces that serve as templates for peptide interactions that do

[†]Acknowledgment is made to the donors of ADR, a program of the American Health Assistance Foundation, for support of this research. This work was also supported by an award from the American Heart Association, National Center (0535185N to V.R.), and Robert and Clarice Smith Fellowship awards (to B.D.M. and W.M.T.).

*To whom correspondence should be addressed. Telephone: (904) 953-7375. Fax: (904) 953-7370. E-mail: rosenberry@mayo.edu.

[1]Abbreviations: AD, Alzheimer's disease; ADDLs, amyloid-derived diffusible ligands; AFM, atomic force microscopy; CD, circular dichroism; ESI, electrospray ionization; EM, electron microscopy; 2−4mers, dimer, trimer, and tetramer forms of Aβ(1−42); LDS, lithium dodecyl sulfate; MALDI, matrix-assisted laser desorption ionization; MALS, multiangle light scattering; MS, mass spectrometry; PAGE, polyacrylamide gel electrophoresis; PBS, 150 mM NaCl and 25 mM sodium phosphate (pH 7.0); SDS, sodium dodecyl sulfate; SEC, size exclusion chromatography; TGase, transglutaminase.

 Published on Web 11/05/2009

not readily occur in aqueous buffers in vitro. Previous studies have shown that both anionic micelles composed of gangliosides and reconstituted liposomes that resemble cellular lipid rafts promote Aβ binding and β-structure formation (*15*−*18*). We have demonstrated that polar−nonpolar interfaces formed in dilute hexafluoro-2-propanol (*19*) and aqueous solution/chloroform mixtures (*20*) promote aggregation of Aβ and its conversion to β-structure. In addition, we found that anionic micelles formed at low concentrations of SDS have strikingly different effects on the aggregation of Aβ(1−40) and Aβ(1−42). In 2 mM SDS, Aβ(1−40) slowly generated large soluble fibers (*13*), but Aβ(1−42) rapidly formed small soluble oligomers that converted to larger "globulomers" (*21*) following dialysis (*14*). While these oligomers gave bands on SDS−PAGE immunoblots with sizes that resembled those of the endogenous aggregates noted above, the synthetic and endogenous oligomers show clear differences in size and stability. In particular, the synthetic oligomers do not elute as discrete dimers through dodecamers on SEC, and they are completely disaggregated by being boiled in 1% SDS. One possible explanation for this difference is that endogenous oligomers are stabilized by covalent cross-linking induced by unknown cellular agents. Previous reports have suggested that cross-linked Aβ dimers and tetramers are found in extracts of AD brains (*22*, *23*), and several agents have been shown to generate Aβ oligomers in vitro that are stable to boiling in SDS, presumably by promoting covalent intermolecular cross-linking. These include copper in the form of Cu(II) (*24*, *25*), TGase (*26*, *27*), prostaglandin products of cyclooxygenase (*28*, *29*), and 4-hydroxynonenal (*30*). These cross-linking agents could also be important in a physiological context, particularly if they were concentrated near cellular interfaces that promoted Aβ aggregation.

The most direct demonstration of covalent cross-linking of endogenous Aβ would involve structural analyses by mass spectrometry (MS), but the low levels of Aβ oligomers in vivo make such characterization an extremely difficult technical task. Optimal cross-linked oligomer isolation and MS analysis procedures need to be developed, and this optimization is more easily conducted with aggregates produced from synthetic Aβ and subjected to several cross-linking procedures in vitro. We begin this process here with fibrillar, oligomeric, and monomeric Aβ(1−42) by comparing the efficiency of covalent cross-linking, the effect of cross-linking on peptide secondary structure, the stability of the cross-linked structures to thermal unfolding, and the sites of peptide cross-linking obtained from proteolysis and MS. In these initial efforts, we have not tried to guess which cross-linking agent might be involved in cross-linking in vivo but instead have selected three different cross-linking agents, TGase, glutaraldehyde, and Cu(II) with peroxide, whose sites of reaction on peptides are well-defined. These agents are among those previously shown to cross-link Aβ in vitro. TGase catalyzes formation of a covalent bond between the free ε-amino group of a lysine residue and the γ-carboxamide group of glutamine residue. Endogenous TGase plays important roles in apoptosis, cellular differentiation, and matrix stabilization, and TGase-catalyzed cross-links colocalize with Aβ in senile plaques in the brains of AD patients (*31*). Glutaraldehyde is a homobifunctional amine cross-linker that generates a range of cross-linked Aβ species (*32*). Cu(II) also induces Aβ cross-linking in the presence of hydrogen peroxide. Cu(II) with peroxide promotes dityrosine cross-linking of Aβ to generate oligomers (*25*).

EXPERIMENTAL PROCEDURES

Materials. Aβ(1−42) was synthesized utilizing orthogonal Fmoc solid phase chemistry by the Peptide Synthesis Facility at the Mayo Clinic (Rochester, MN) as described previously (*14*). MS revealed >90% purity. SDS, bovine serum albumin, and thioflavin T were procured from Sigma (St. Louis, MO). All other buffers and salts were obtained from Fisher Inc.

Preparation of Aβ Monomer. Lyophilized Aβ(1−42), stored desiccated at −80 °C, was dissolved at concentrations of 0.5−2.0 mM in 30 mM NaOH (*33*). Monomers were isolated by size exclusion chromatography (SEC) on a Superdex 75 HR 10/30 column (Amersham Pharmacia) equilibrated in 20 mM Tris-HCl (pH 8.0) and run at a flow rate of 0.5 mL/min (*14*). Peptide integrity was again confirmed by ESI-MS.

Aggregation of Aβ(1−42). All reactions were initiated in siliconized Eppendorf tubes. Fibrils were prepared by incubation of monomeric Aβ(1−42) (50 μM) in 20 mM Tris-HCl (pH 8.0) with 150 mM NaCl at 37 °C for 2−5 days. Fibril formation was confirmed by thioflavin T fluorescence (*12*, *34*). Fibrils were pelleted by centrifugation at 18000*g* for 10 min, washed with water, and resuspended in 10 mM Tris-HCl (pH 8.0). The Aβ(1−42) 2−4mers were generated by incubation of monomeric Aβ(1−42) in 10 mM Tris-HCl (pH 8.0), 50 mM NaCl, and dilute SDS for 16−24 h at 25 °C. Two incubation conditions were used: 25 μM Aβ(1−42) in 2 mM SDS (*14*) or 100 μM Aβ(1−42) in 4 mM SDS. Aβ(1−42) oligomers were formed by dialysis of a 2−4mer preparation against 10 mM Tris-HCl (pH 8.0) for 48 h at 25 °C in the absence of SDS, and any large aggregate contaminants were removed by centrifugation (18000*g* for 10 min) (*14*). Unless otherwise noted, all oligomer preparations here were generated from 100 μM 2−4mers and purified by SEC on Superdex 75 column as indicated for monomers above. Concentrations of all Aβ species were determined by UV absorbance with a calculated extinction coefficient of 1450 cm^{-1} M^{-1} at 276 nm (*12*), and all Aβ aggregate concentrations are expressed in monomer units.

Multiangle Light Scattering (*MALS*). Samples were applied to a Superdex 75 SEC column attached to an AKTA FPLC system and analyzed in-line with a DAWN EOS MALS instrument using ASTRA for Windows 4.90.04 (Wyatt Technology, Santa Barbara, CA) (*12*, *19*). The analysis was based on the Zimm formalism of the Rayleigh−Debye−Gans model (*35*, *36*), as presented previously (*12*). In brief, the excess Rayleigh ratio (R_θ) is related to the molecular structure according to eq 1

$$\frac{Kc}{R_\theta} = \frac{1}{MP(\theta)} + 2A_2c \qquad (1)$$

where R_θ is proportional to the fraction of incident light that is scattered by the solute without interference; K is a physical constant equal to $4\pi^2(dn/dc)^2 n_o^2 N_A^{-1} \lambda_o^{-4}$, where n is the refractive index of the solution, c is the solute concentration (grams per milliliter), n_o is the refractive index of the solvent, N_A is Avogadro's number, and λ_o is the wavelength of the incident light in vacuum; A_2 is the second virial coefficient; and M is the molecular mass of the solute. At the low concentrations c employed in this study, the $2A_2c$ term in eq 1 may be ignored. The function $P(\theta)$ is the ratio of the scattered light intensity to the scattered light intensity without interference. For bovine serum albumin and the relatively small peptide aggregates here, R_θ showed no angular dependence and $P(\theta)$ was set to 1. In calibration runs with bovine serum albumin, the monomer peak was preceded by a small shoulder of dimer, and the M for

monomer was determined to be 76 ± 1 kDa (average of four SEC experiments).

Cross-Linking. Aβ(1−42) species (15−20 μM) were treated with three cross-linking agents under the following conditions. TGase (from guinea pig liver, 2 units/mg, Sigma-Aldrich) was added to a final concentration of 4, 20, or 100 μg/mL in 10−50 mM Tris-HCl (pH 8.0) with 5 mM $CaCl_2$ for 30 min at 37 °C. Glutaraldehyde at 0.002, 0.01, or 0.05% in 5−10 mM Tris-HCl (pH 8.0) was incubated with Aβ samples for 15 min, and sodium cyanoborohydride was then added to a final concentration of 40 mM for an additional 15 min at 25 °C. The reaction was quenched by the addition of 1 M Tris to a final concentration of 80 mM. $CuCl_2$ (25 μM), 50, 250, or 1250 μM H_2O_2, and 150 mM NaCl were incubated with Aβ overnight at 37 °C.

Polyacrylamide Gel Electrophoreses (*PAGE*) *and Immunoblotting*. Samples were adjusted to loading buffer (NuPAGE, Invitrogen Inc., Carlsbad, CA) containing 2% LDS, either maintained at 25 °C or boiled for 3−5 min as indicated, applied to NuPAGE precast 4 to 12% acrylamide gels containing bis-Tris, and resolved in NuPAGE MES SDS running buffer with 0.1% SDS. Dye-linked *M* markers (SeeBlue Plus2 Prestained Standards, Invitrogen) were run in parallel for calibration. In some cases, gels were stained with silver (Pierce SilverSNAP Stain Kit II). Relative intensities of silver-stained bands were determined by densitometry after brief staining periods that avoided band saturation (*37*). In other cases, gels were electroblotted onto 0.2 μm nitrocellulose membranes (Bio-Rad, Hercules, CA), and blots were boiled for 10 min in PBS. After an overnight incubation with blocking buffer (0.5× PBS, 0.5% casein, and 0.01% thimerosal), the blots were probed with monoclonal antibody Ab9 (*38*), which recognizes an epitope in Aβ(1−16). Blots were then incubated with a goat anti-mouse antibody conjugated to fluorophore 680 (Invitrogen) and scanned by Odyssey (LI-COR Biosciences, Lincoln, NE). Intensities of bands on the blot were quantified using Odyssey version 2.1.

Circular Dichroism (*CD*) *Spectroscopy*. CD spectra were recorded in the far-UV region with a Jasco J-810 spectropolarimeter (Jasco Inc., Easton, MD) in continuous scan mode (260−190 nm) and a 0.1 cm path length quartz cuvette (Hellma) as described previously (*14*). The temperature dependence of the spectra was acquired by programming the Peltier temperature controller as follows. After initial spectra were collected in triplicate at 20 °C, the temperature was increased to 30 °C and the sample was equilibrated for 2 min prior to again recording the spectra in triplicate. This cycle was repeated in succession for the following temperatures: 40, 50, 60, 70, 80, 90, and 100 °C. Spectra of appropriate blanks (all components except Aβ) were subtracted from the data sets.[2] The corrected, averaged spectra were smoothed (*14*) and converted to mean residue ellipticity with the equation $[\theta] = [\theta]_{obs}(MRW/10lc)$, where MRW is the mean residue molecular weight of Aβ(1−42) (4514 g/mol divided by 42 residues), l is the optical path length (centimeters), and c is the concentration (grams per cubic centimeter). The temperature (T) dependence was expressed as the difference in ellipticity values between 208 and 218 nm ($\Delta[\theta] = [\theta]_{208} - [\theta]_{218}$) and fitted (SigmaPlot 11) to the sigmoidal curve in eq 2 (*39*).

$$[\theta]_{208} - [\theta]_{218} = \Delta[\theta]_L + \frac{\Delta[\theta]_H - \Delta[\theta]_L}{1 + e^{-[(T - T_M)/W]}} \quad (2)$$

with four variable parameters ($\Delta[\theta]_L$, $\Delta[\theta]_H$, T_M, and W), where $\Delta[\theta]_L = [\theta]_{208} - [\theta]_{218}$ at low temperatures, $\Delta[\theta]_H = [\theta]_{208} - [\theta]_{218}$ at high temperatures, T_M is the temperature at which the spectra are 50% converted, and W is a measure of the breadth of temperatures over which the conversion occurs. This difference is positive for β-structure and negative for α-helical structure.

Pepsin Digestion. Aβ samples (20−25 μM) to be digested with pepsin were adjusted to pH 2 with trifluoroacetic acid, and porcine pepsin (Sigma Aldrich) was added to a final concentration of 10 μg/mL. Samples were incubated for 2 h at 37 °C with periodic brief shaking and then diluted 2−10-fold with water for MS analysis.

Mass Spectrometry. A Bio-Rad ProteinChip System Series 4000 (Enterprise Edition) mass spectrometer was used in MALDI-TOF mode. Samples were mixed in equal volume with the energy absorbing matrix [sinapinic acid (Acros) (25 mg/mL) in 50% acetonitrile and 0.5% trifluoroacetic acid], and 1 μL (corresponding to 1−5 pmol of Aβ) was spotted on a ProteinChip Gold Array (A-H Format). The laser intensity was adjusted to 3000 nJ.

ESI-MS analyses were conducted with a ThermoFinnigan DecaXP Plus ion trap mass spectrometer equipped with a NanoMate 100 automated nanoelectrospray injection accessory.

RESULTS AND DISCUSSION

Isolation and Mass Determination for Distinct Aβ Oligomers. Isolated monomeric forms of Aβ(1−40) and Aβ(1−42) aggregate to fibrils when incubated in aqueous buffers. Under identical conditions and equivalent Aβ concentrations, the rate of fibril formation is several-fold higher with Aβ(1−42) than with Aβ(1−40), but the fibrils formed by both peptides appear to be similar as determined by electron microscopy (EM) and atomic force microscopy (AFM) and exhibit predominant β-structure by circular dichroism (CD) (*13*, *14*). When anionic micelles formed by 2 mM sodium dodecyl sulfate (SDS) are included in these reactions, the micellar interface accelerates the generation of fibers by Aβ(1−40) but induces the immediate formation of small nonfibrillar aggregates by Aβ(1−42) (*14*, *21*). We have denoted these small aggregates 2−4mers because they typically migrate as a doublet of bands in the 8−14 kDa region on SDS−PAGE gels, in contrast to the single 4 kDa band observed with isolated Aβ(1−42) monomers (Figure 1A). Dialysis of the 2−4mers to remove SDS preserves the aggregated state in a form that we denote oligomers and Barghorn et al. have termed globulomers (*21*). SDS−PAGE of these oligomers reveals a broad band centered at ~40 kDa in addition to 2−4mer and monomer bands (Figure 1A). Oligomers also exhibit predominant β-structure by CD and appear as globular particles with an average height of 1.9 nm on AFM, a height similar to those of 2−4mers and isolated monomers (*14*). Boiling samples of 2−4mers, oligomers, or fibrils in SDS−PAGE sample buffer prior to SDS−PAGE converts all Aβ species to monomers [Figure 1B (*14*)]. Quantitative distributions of the Aβ(1−42) peptide among the SDS−PAGE bands from these aggregates are difficult to assess because relative immunoblot band intensities with antibody Ab9 depend on

[2]For example, complete CD spectra for temperature melts with TGase and without Aβ were recorded as blanks for the spectra depicted in Figure 6A. The TGase correction was minimal. TGase primarily exhibited an α-helical conformation on CD, and at 20 μg/mL, the TGase CD profile was barely above the buffer baseline. This background was incorporated by subtracting it from the raw CD spectra with Aβ prior to conversion to mean residue ellipticity.

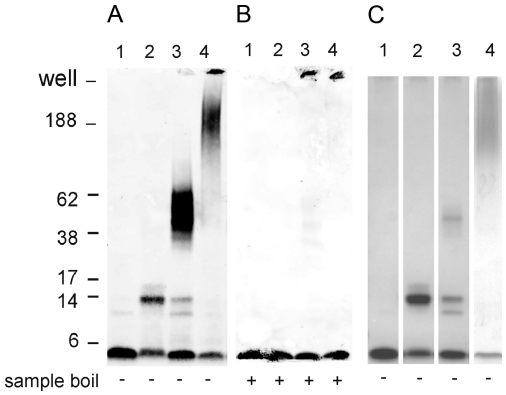

FIGURE 1: Variation in band intensities of Aβ(1−42) samples following SDS−PAGE analysis. Lanes 1−4 correspond to monomer, 2−4mer, oligomer purified by SEC as shown in Figure 2A, and fibril, respectively (30 pmol), that were run in triplicate before immunoblotting (A and B) or gel staining with silver (C). The samples in gel B were boiled in sample buffer prior to SDS−PAGE, while those in gel A were not.

whether the blot has been boiled (*14*) and differ from immunoblot band intensities with antibody 6E10 (*14*) and from gel band intensities obtained by silver staining. In particular, immunostaining of Aβ aggregates is enhanced relative to that indicated by silver staining (e.g., note the differences in relative band intensities between identical samples in lane 3 of Figure 1A and lane 3 of Figure 1C).

The conversion of monomers to 2−4mers and then to oligomers with these procedures does not proceed quite to completion. Residual monomers remain after the dialysis step used to generate oligomers, and CD spectra showed variations among preparations in their relative β-structure content. Initial attempts to separate the dialyzed oligomers from residual monomers by SEC were unsuccessful because very little oligomer was recovered. However, scaling up the overnight incubation from 25 μM Aβ(1−42) in 2 mM SDS to 100 μM Aβ(1−42) in 4 mM SDS preserved a high yield of 2−4mers, and following dialysis, an oligomer peak was well separated from the residual monomer peak on SEC (Figure 2A). The overall Aβ recovery from this SEC (~70%) still indicated some oligomer loss due to adsorption on the column matrix, but the recovery was sufficient for examination of whether any size fractionation of the oligomers themselves was obtained. Fractions between the peaks in Figure 2A were analyzed by SDS−PAGE, but no separation of discrete species, from apparent nonamers in the ~40 kDa bands to apparent dimers and trimers in the 2−4mer bands, was obtained (Figure 2B). Densitometric scans revealed a constant ratio of ~40 kDa, 2−4mer, and monomer bands in fractions 21−27, a pattern broken only by a more intense monomer band as the monomer peak in fraction 33 was approached. This result indicates that the dialyzed oligomers elute as a single species on SEC but that this species is partially dissociated to an ~40 kDa aggregate as well as 2−4mers and monomers in the 1% LDS loading buffer at room temperature prior to SDS−PAGE. We previously reached a similar conclusion about the stability of Aβ(1−42) aggregates generated in vitro in the absence of SDS (*14*). To estimate the molecular mass M of the oligomeric aggregate centered at fraction 21, we monitored the SEC eluent by MALS to obtain a continuous record of M (Figure 2A). Following a small amount of larger aggregates near the void volume, the oligomer peak was characterized by a nearly constant M that averaged 150 ± 18 kDa (average of four SEC experiments).

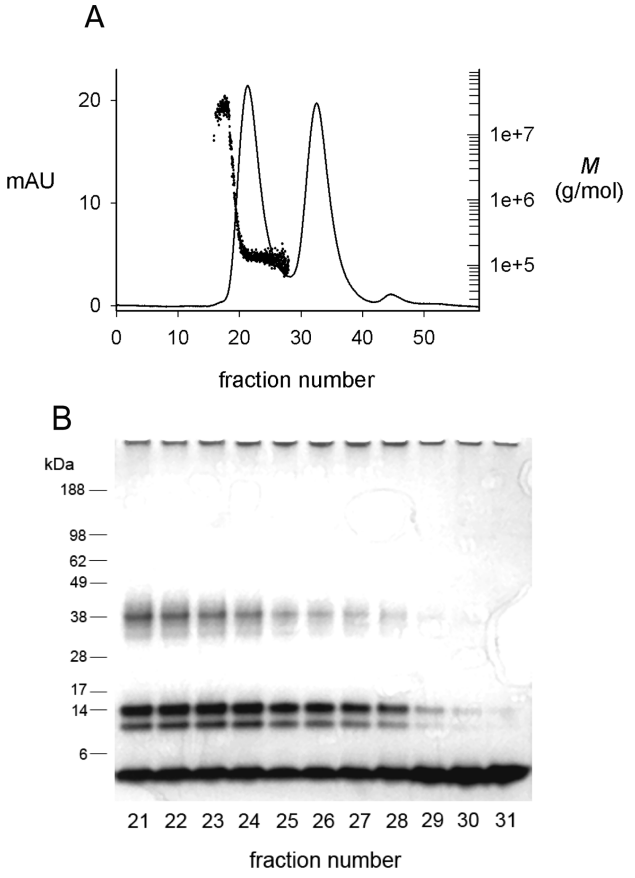

FIGURE 2: Fractionation of dialyzed Aβ(1−42) oligomers by SEC. SEC-purified Aβ(1−42) monomers (100 μM) were incubated in 4 mM SDS for 20 h and dialyzed against 10 mM Tris-HCl (pH 8.0) for 48 h at 25 °C to generate oligomers. (A) A 2 mL sample was applied to Superdex 75 equilibrated in 20 mM Tris-HCl (pH 8.0), and elution was monitored online by simultaneous recording of the absorbance at 280 nm (mAU = absorbance/1000, solid line) and MALS. Calculations of M were based on eq 1 as outlined in the Experimental Procedures (dots). Peaks at fractions 21 (near the void volume) and 33 corresponded to oligomers and monomers, respectively. The total Aβ recovery (A_{280}) was 70%. (B) Samples from the indicated fractions in panel A (50 pmol) were mixed with SDS gel loading buffer at 25 °C for PAGE analysis. The gel was stained with silver to eliminate intense immunoblotting of the largest oligomeric band (see Figure 1).

A number of soluble Aβ aggregates formed in vitro from synthetic Aβ monomers in vitro have been reported. These include protofibrils (*12*, *40*−*42*), amyloid-derived diffusible ligands (or ADDLs) (*6*), and oligomers or globulomers generated from Aβ(1−42) in dilute SDS (*14*, *21*). A few groups have reported sizes of these soluble Aβ aggregates based on a combination of SEC and MALS to determine the M values. Protofibrils of Aβ(1−40) were quite large and had initial M values of 7−30 × 10^3 kDa (*12*). ADDLs, which are formed only by Aβ(1−42), displayed a polydisperse SEC peak that ranged in size from 150 kDa at the trailing edge to nearly 1 × 10^3 kDa at the leading edge (*43*). The lower M range of these ADDLs thus corresponds closely to that of the oligomers shown in Figure 2A. However, the oligomers here appeared to be more homogeneous, as the M of 150 kDa was nearly constant across the entire aggregate peak in Figure 2A, and this peak was preceded by only a small amount of larger aggregates near the void volume. In addition, the ratio of oligomers to monomers based on UV absorbance in Figure 2A was higher than that shown for the ADDL preparation. Aβ(1−42) globulomers generated in dilute

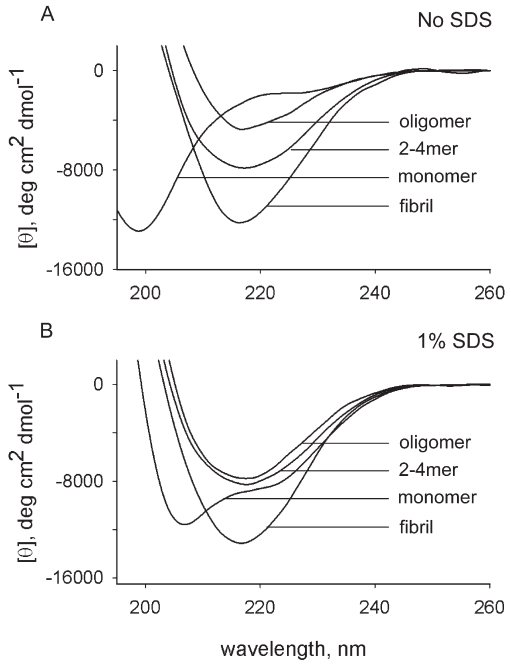

FIGURE 3: CD spectra of various Aβ(1−42) species in the presence and absence of 1% SDS. Aβ species (15−25 μM) in 10−20 mM Tris-HCl (pH 8.0) (A) or the same buffer with 1.0% SDS (B) were generated as described in Experimental Procedures, and spectra were recorded at 20 °C. (A) The monomer spectra corresponded to a typical random coil structure with no minima above 200 nm, while the three aggregates show a predominant β-structure with a characteristic minimum at 218 nm. (B) Addition of SDS converted the monomers to a predominant α-helical structure with characteristic minima near 208 and 222 nm. Spectra of the three aggregates were essentially unchanged by addition of SDS at 20 °C.

SDS were recently reported to have a molecular mass of 64 kDa by analytical ultracentrifugation analysis (*44*). These reports are noteworthy in their failure to detect discrete small oligomers in the dimer to dodecamer size range analogous to those observed by SEC for endogenous Aβ oligomers. However, Figure 2B revealed that SDS−PAGE bands in this dimer to dodecamer size range are generated by partial dissociation of the 150 kDa oligomers in LDS sample buffer. Therefore, caution is advised in assuming that oligomer sizes determined from SDS−PAGE gel bands correspond to native molecular masses in the absence of SDS.

Thermal Stability of Aβ(1−42) Aggregates in 1% SDS. Aβ monomers show little secondary structure and give CD spectra dominated by a random coil configuration (Figure 3A). In contrast, Aβ(1−42) fibrils, 2−4mers, and oligomers each exhibit predominant β-structure based on a CD minimum at 218 nm that is characteristic of β-structure, but the different mean residue ellipticity values at 218 nm indicate a higher extent of β-structure formation in fibrils than in 2−4mers or oligomers (Figure 3A). To gain further insight into structural differences among these Aβ(1−42) aggregates, we compared their stabilities in 1% SDS. The measurement of secondary structure changes by CD in 1% SDS has a number of advantages. First, it allows direct comparison to SDS−PAGE analyses because SDS−PAGE onput samples typically contain 1−2% SDS or LDS. Second, monomeric Aβ(1−42) like many other proteins (*45*) is rapidly converted to a predominant α-helical structure in 1% SDS (compare monomer spectra in panels A and B of Figure 3). The CD spectrum of monomeric Aβ(1−42) in 1% SDS at 20 °C exhibits minima near 208 and 222 nm that are characteristic of an α-helical conformation and readily distinguished from a spectrum with predominant β-structure. Third, 1% SDS acts as a denaturant that converts less stable β-structures to α-helices but leaves more stable β-structures unaltered. Therefore, stability as a function of temperature can be determined by "temperature melt" experiments in which CD spectra are recorded in 1% SDS at progressively higher temperatures. Finally, the α-helical spectra of Aβ(1−42) after complete disruption of β-structure in 1% SDS at high temperature show the same mean residue ellipticity values at 208 and 222 nm regardless of the initial aggregate structure. This is particularly helpful in normalizing Aβ concentrations.

The Aβ(1−42) aggregate samples in Figure 1A show little disaggregation to monomer upon addition of LDS to 2% at room temperature prior to SDS−PAGE, so it is not surprising that CD spectra in Figure 3B show retention of most β-structure in the aggregates in 1% SDS at 20 °C. However, the oligomeric and higher aggregate bands observed for Aβ(1−42) 2−4mers, oligomers, or fibrils are all converted to a monomer band when samples are boiled for 5 min in 2% LDS sample buffer prior to SDS−PAGE [Figure 1B; (*14*)]. Boiling in 1% SDS also converts these aggregated samples to predominant α-helical structures as measured by CD. This conversion is irreversible, as the CD spectra remain characteristic of an α-helical structure after the samples are cooled to 20 °C. To monitor the temperature dependence of the conversion, we recorded successive CD spectra at increasing 10 °C temperature intervals in 1% SDS. Panels A and B of Figure 4 show selected spectra from such progressive

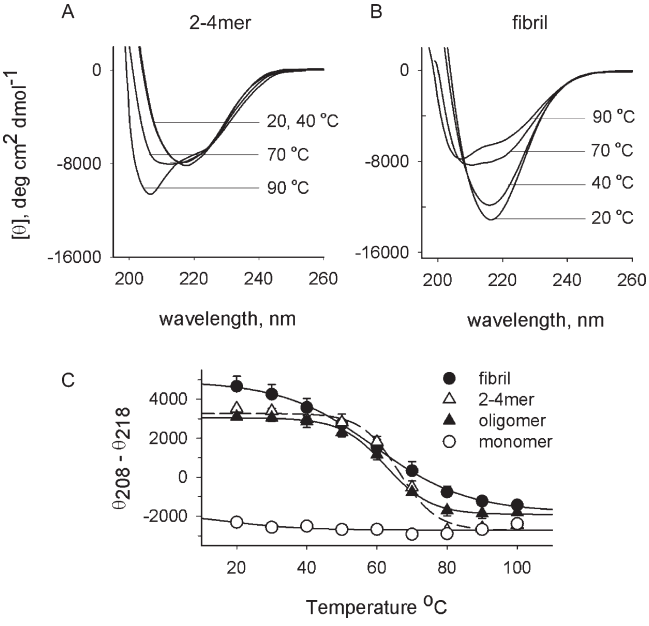

FIGURE 4: Temperature dependence of CD spectra for various Aβ(1−42) species in 1.0% SDS. SDS was added to Aβ(1−42) samples (15−20 μM) to a final concentration of 1.0%, and consecutive spectra were recorded at increasing temperatures as described in Experimental Procedures. Representative spectra are shown for 2−4mers (A) and fibrils (B). Spectra for oligomers (not shown) were very similar to those of 2−4mers. (C) Individual temperature melts indicate relative β-structure ($[\theta]_{208} - [\theta]_{218}$) as a function of temperature for monomer (○), 2−4mer (△ and dashed line), oligomers (▲), and fibrils (●) (points are averages of four or five experiments). Lines were calculated with eq 2. Average values of T_M and W from eq 2 were 59 ± 3 and 12 ± 1 °C for fibrils, 66 ± 1 and 5 ± 1 °C for 2−4mers, and 63 ± 1 and 6 ± 1 °C for oligomers, respectively. The Aβ(1−42) monomer did not exhibit substantial spectral changes with temperature since it is already converted to an α-helical structure at 20 °C, as shown in Figure 3B.

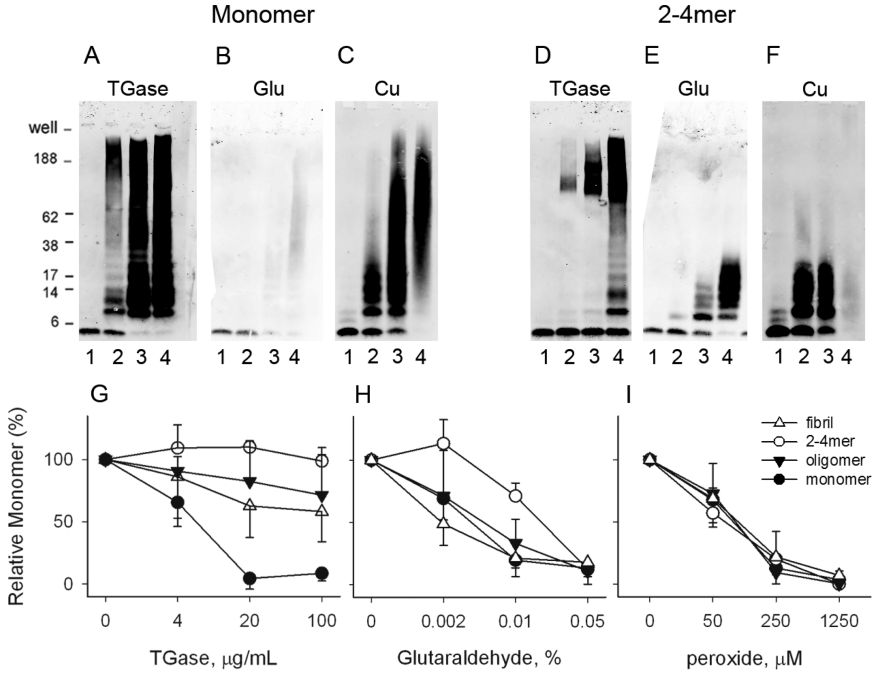

FIGURE 5: Cross-linking of various Aβ(1−42) species with three cross-linking agents. Aβ samples were treated without and with three concentrations of each indicated cross-linking agent, boiled in 2% LDS, and analyzed by SDS−PAGE and immunoblotting with antibody Ab9 as outlined in Experimental Procedures. The concentrations of each agent examined are given in panels G−I, and immunoblots of treated samples (with agent concentrations increasing from lanes 1 to 4) are shown in panels A−F. The procedure is illustrated with Aβ monomers (A−C) and 2−4mers (D−F). Immunoblots of Aβ oligomers and fibrils (not shown) showed cross-linked oligomeric bands, primarily in the 100−200 kDa range, with all three cross-linking agents. The extent of cross-linking was quantified by the relative intensity of the monomeric band using Odyssey LI-COR. Intensities of this band in each blot were normalized by setting the intensity of the monomeric band in the absence of cross-linking agent to 100%. Panels G−I show relative band intensities for monomer (●), 2−4mer (○), oligomers (▼), and fibrils (△) at each cross-linking agent concentration. Oligomers in these experiments were dialyzed samples prior to SEC purification. Points are averages of three or four measurements.

temperature melts of Aβ(1−42) 2−4mers and fibrils, respectively. As expected from Figure 3B, both species begin at 20 °C with predominant β-structure but are converted to α-helical structures as the temperature increases. Since the spectra were recorded only 2 min after each step in temperature, the changes in spectra largely reflected the kinetics of thermal refolding. A similar procedure was used to reveal differences in the temperature dependence of unfolding between two alternative conformations of a yeast prion protein (*39*), and we examined whether differences could also be observed among these aggregated Aβ(1−42) samples. Relative secondary structure was quantified as the difference in mean residue ellipticity between 208 and 218 nm ($\Delta[\theta] = [\theta]_{208} - [\theta]_{218}$). This difference is positive when β-structure predominates but decreases to negative values as the structure is converted to α-helix. Values of $\Delta[\theta]$ at 20 °C in Figure 4C are larger for fibrils than for 2−4mers or oligomers, indicating a greater level of relative β-structure in fibrils at this temperature. The T_M at which 50% conversion to α-helical structure occurred (59−66 °C) was similar for all three aggregates, but differences were observed in the temperature range over which the conversion occurred. If this range is defined by 5−95% conversion (corresponding to $6W$ in eq 2), the range for 2−4mers was 30 °C, that for oligomers was 38 °C, and that for fibrils was 72 °C, essentially the entire 30−100 °C span. In fact, some residual β-structure in fibril samples was suggested by the plot in Figure 4C even after the final step at 100 °C. We concluded that the region of β-structure in 2−4mers and oligomers was quite homogeneous, whereas fibrils have heterogeneous regions of β-structure that are disrupted by heating in 1% SDS at quite different rates. These observations indicate structural differences in the β-structured regions in 2−4mers and oligomers relative to fibrils.

Cross-Linking Efficiency Varies with the Aβ(1−42) Species and the Cross-Linking Agent. The aggregation of Aβ into fibrils or the association of Aβ in oligomers at SDS micelle interfaces could have two opposing effects on the efficiency of cross-linking reactions. Cross-linking could be enhanced by bringing reactive groups on adjacent peptides into closer contact. Alternatively, cross-linking could be inhibited because reactive groups are buried within the region of peptide contact and inaccessible to the cross-linking agent. To examine which effect predominates with the three cross-linking agents employed in this study, samples were prepared over a range of cross-linking agent concentrations and examined by SDS−PAGE and immunoblotting (Figure 5). Samples were boiled prior to SDS−PAGE to preserve only covalently linked oligomeric bands. While immunoblotting provides the most sensitive measure of the conversion of Aβ monomers to higher-order oligomers, quantifying band intensities on these blots can be confounded in several ways. We noted above that relative band intensities with antibody Ab9 (1) depend on whether blots have been boiled and (2) differ from the relative intensities of bands on corresponding silver-stained gels (Figure 1). We therefore focused just on the relative intensities of monomer bands in boiled blots to assess the extent of intermolecular cross-linking. For example, panels A and D of Figure 5 compare immunoblots of monomers and 2−4mers cross-linked by TGase. Many bands with masses greater than 4 kDa are apparent, and the intensities of these bands appear to be greater in the monomer sample than in the 2−4mer sample. This impression is supported by

quantitative analysis of the relative monomer band intensities in Figure 5G. Monomer bands in the blots of the cross-linked monomer sample are barely detectable at the two highest TGase concentrations, while these bands from the 2−4mer as well as fibril and oligomer samples retain at least 50% of the intensity of the non-cross-linked control at all TGase concentrations. These data indicate that Aβ monomers were cross-linked by TGase more efficiently than any of the three Aβ aggregates examined here. Panels A and D of Figure 5 also illustrate a second concern in immunoblot interpretation when the cross-linking agent is itself a protein. Immunostained bands near 100 kDa increase in rough proportion to the amount of TGase in the sample. Hartley et al. (*46*) have reported that TGase cross-links itself to Aβ, and such a cross-link would result in an ~100 kDa band that immunostains for Aβ. To minimize this undesired cross-linking in the remaining experiments here, TGase was limited to the penultimate concentration shown in Figure 5G (20 μg/mL).

Interpretation of immunostaining also may be compromised if the epitope(s) for antibody interaction becomes blocked during the cross-linking reaction. Glutaraldehyde cross-linking resulted in a loss of monomer band immunostaining without a corresponding increase in higher-mass bands (Figure 5B). Silver staining of gels of paired samples, however, showed no decrease in monomer band intensity even at the highest glutaraldehyde concentration (data not shown). MS data below helped to reconcile this discrepancy, as it showed pronounced reactivity of glutaraldehyde with the N-terminal primary amine group of Aβ to form a piperidine conjugate. This modification appears to be sufficient to block the binding of antibody Ab9 and eliminate immunostaining of the modified peptides. The fact that immunostained oligomeric bands were apparent following glutaraldehyde cross-linking of Aβ 2−4mers (Figure 5E) as well as oligomers and fibrils (data not shown) suggests that the N-terminus may become less accessible to glutaraldehyde in aggregated Aβ species.

Cross-linking with Cu(II) and peroxide resulted in covalent oligomeric bands for Aβ monomers (Figure 5C) and 2−4mers (Figure 5F), as well as oligomers and fibrils (data not shown), and the dependence of monomer loss on peroxide concentration was similar for all four Aβ species (Figure 5I). Loss of immunostaining at the highest peroxide concentration (e.g., Figure 5F) may also reflect modification of the epitope for Ab9 binding; however, comparison to silver-stained gels was not informative as the extent of silver staining of the monomer band also decreased at higher peroxide concentrations, and little silver staining of oligomeric bands was apparent (data not shown).

Increased Thermal Stability of Some Cross-Linked Aβ Aggregates. The β-structure inferred for aggregated Aβ(1−42) species from the CD spectra in Figure 3 was largely retained following treatment with all three cross-linking agents. In addition, this β-structure was maintained in the presence of 1% SDS. Temperature melt curves in 1% SDS for fibrils, 2−4mers, and oligomers after treatment with the cross-linking agents are shown in Figure 6, and in general, values of $\Delta[\theta]$ at 20 °C are similar to those in Figure 4C. However, cross-linking did have an effect on some of the curves at higher temperatures in Figure 6. Fibrils exhibited less conversion to α-helical structure at high temperatures after treatment with each of the cross-linking agents, indicating that cross-linking stabilized the fibril β-structure. In fact, it appears that not all Aβ peptides in a fibril need be cross-linked for their β-structure to be influenced by a neighboring cross-linked Aβ. Cross-linking with TGase stabilized most of the fibril β-structure (Figure 6A), even though fewer than half of the monomers in the fibril sample were cross-linked by TGase (Figure 5G). In contrast, the stability of β-structure in 2−4mers and oligomers was not increased by treatment with TGase or Cu(II) with peroxide, as $\Delta[\theta]$ at high temperatures ($\Delta[\theta]_H$ = −1900 to −3100 from Figure 6A,C) was not significantly different from that of 2−4mers and oligomers prior to cross-linking ($\Delta[\theta]_H$ = −1900 to −2700 from Figure 4C). Glutaraldehyde cross-linking preserved more β-structure in 2−4mers and oligomers at high temperatures ($\Delta[\theta]_H$ = 300−600 from Figure 6B).

CD spectra of monomeric Aβ(1−42) in 1% SDS indicated predominant α-helical structures at all temperatures in Figure 4C, and no conformational melt was detected. This melt pattern was retained after treatment of monomers with glutaraldehyde or Cu(II) with peroxide, and a similar level of α-helical

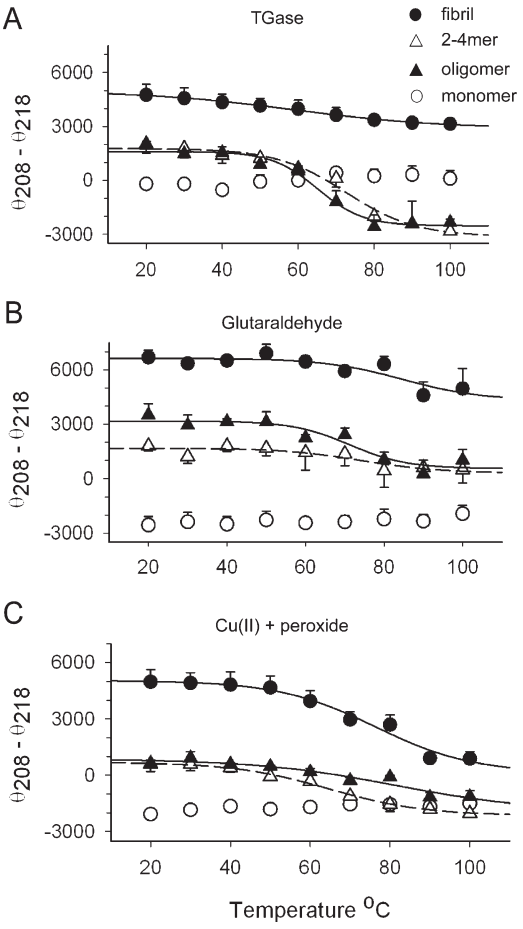

FIGURE 6: Temperature dependence of CD spectra following cross-linking of various Aβ(1−42) species. The Aβ(1−42) species indicated in panel A were cross-linked with (A) TGase (20 μg/mL), (B) glutaraldehyde (0.05%), or (C) Cu(II) with peroxide (1250 μM) as described in the legend of Figure 5, and the temperature dependence of CD spectra of the samples was obtained as described in the legend of Figure 4C. Points are averages of three to five experiments, and lines were calculated with eq 2. Average values of T_M and W from eq 2 for TGase were 63 ± 10 and 20 ± 5 °C for fibrils, 70 ± 3 and 9 ± 3 °C for 2−4mers, and 65 ± 1 and 6 ± 1 °C for oligomers, respectively, and for glutaraldehyde 72 ± 5 and 12 ± 7 °C for oligomers, respectively. Equation 2 could not fit the glutaraldehyde data for fibrils or 2−4mers unless one parameter was fixed, and the lines shown were fit with a W of 10 °C. Average values of T_M and W from eq 2 for Cu(II) with peroxide were 76 ± 6 and 12 ± 4 °C for fibrils, 67 ± 3 and 14 ± 6 °C for 2−4mers, and 81 ± 24 and 18 ± 16 °C for oligomers, respectively.

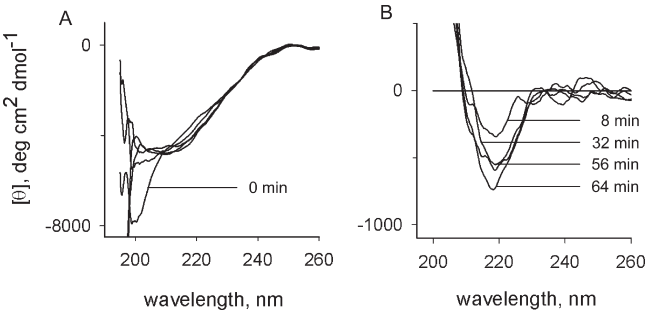

FIGURE 7: Time dependence of transglutaminase cross-linking of Aβ(1−42) monomers. Aβ(1−42) monomer (20 μM) was incubated with 20 μg/mL TGase in 50 mM Tris-HCl (pH 8.0) at 37 °C as described in the legend of Figure 5, and CD spectra were collected every 8 min for 1 h. (A) Spectra recorded at 0, 8, 32, 56, and 60 min (see panel B). (B) Difference spectra obtained by subtracting each spectrum in panel A from the spectrum recorded at the beginning of the incubation (0 min).

structure was preserved ($\Delta[\theta]$ = −1700 to −2300 from Figure 6B,C). However, treatment of monomers with TGase resulted in partial formation of β-structure, as indicated by an increase in $\Delta[\theta]$ to an average of 0 over the course of the melt (Figure 6A), and this β-structure remained stable at high temperatures. To examine the effect of TGase on monomeric Aβ(1−42) more closely, the time course of progressive monomer treatment with TGase was monitored by CD as shown in Figure 7A. The spectra indicate that the monomer initially corresponded to a random coil at the start of the incubation but began to convert to β-structure by 8 min. The conversion is shown more clearly in the difference spectra in Figure 7B. Only a slight further increase in the level of β-structure was observed after 32 min.

Identification of Aβ Residues Modified or Cross-Linked during Cross-Linking Reactions. Cross-linking agents highly specific to certain residues should prescribe a well-defined set of potential cross-links in Aβ(1−42). For example, with TGase, the specific linking of lysine and glutamine side chains requires that cross-linking in Aβ(1−42) be limited to Lys_{16} and/or Lys_{28} and Gln_{15}. A convenient method for identifying cross-linked residues involves specific proteolytic fragmentation followed by MS, because cross-linked peptide fragments can be identified from masses that are distinct from those of fragments obtained in the absence of cross-linking. Proteolysis of Aβ peptides has been investigated (*47*, *48*), and pepsin has been found to cleave preferentially between Phe_{19} and Phe_{20}, between Leu_{34} and Met_{35}, and between Glu_3 and Phe_4 (*48*). We verified these cleavages following pepsin digestion of monomeric Aβ(1−42). The three most prominent peptic fragments observed with MALDI-TOF MS were Aβ(1−19) [$(M + H)^+$ = 2315 Da], Aβ(4−19) (2000 Da), and Aβ(20−34) (1492 Da) (Figure 8B), and these assignments were confirmed by MS/MS analysis with ESI-MS. Pepsin cleaved virtually all of the monomer, as no peak was observed corresponding to intact Aβ(1−42) [$(M + H)^+$ = 4515 in the control in Figure 8A]. We also examined proteolytic fragments of Aβ produced by pepsin digestion after treatment with cross-linking agents. Following cross-linking of monomeric Aβ(1−42) with TGase, pepsin digestion produced two additional species at 3474 and 3983 Da (Figure 8C). These species allowed us to identify the residues involved in the cross-linkage. Since TGase cross-links Lys and Gln residues, Aβ42 cross-links could involve Gln_{15} to Lys_{16} or Gln_{15} to Lys_{28}. The 3474 Da peak corresponded to Aβ(4−19) linked to Aβ(20−34) [$(M + H)^+$ = 3474], and the

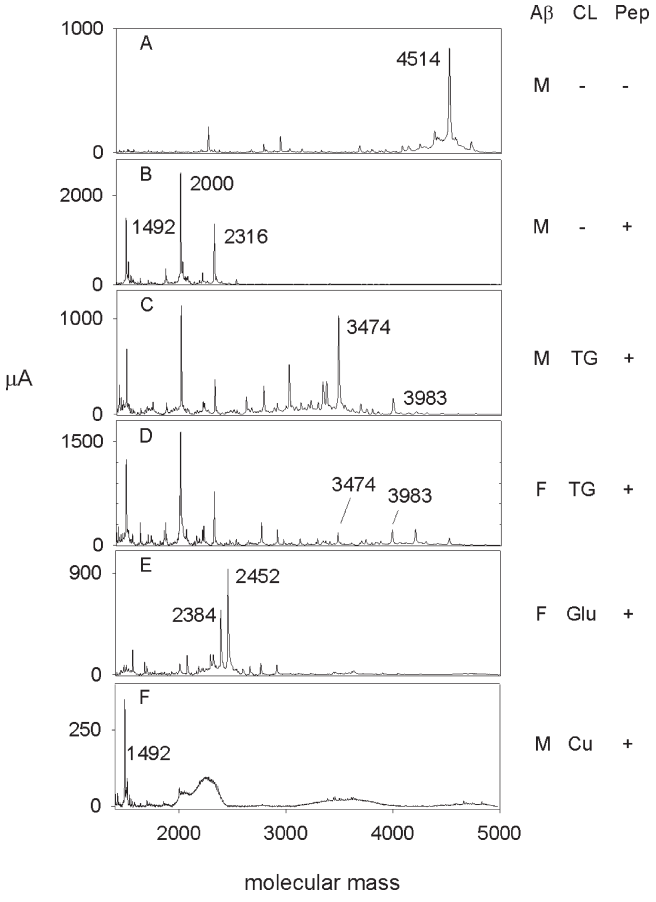

FIGURE 8: MALDI-TOF mass spectrometry analysis of peptic fragments of Aβ(1−42) species before and after cross-linking. Samples of Aβ(1−42) treated with cross-linking agents as described in the legend of Figure 5 or untreated were adjusted to pH 2 and incubated with pepsin as outlined in Experimental Procedures. Aliquots were then mixed with matrix for mass spectrometry. (A−F) Right-hand columns indicate the Aβ species (monomer, M; fibril, F), the cross-linking agent CL [no cross-linking, −; TGase, TG; glutaraldehyde, Glu; Cu(II) with peroxide, Cu], and treatment with pepsin Pep (+) or without (−). The *y*-axis denotes ion current, and numbers in panels show observed molecular masses of indicated peaks.

mass of 3983 indicated Aβ(4−19) linked to Aβ(4−19) [$(M + H)^+$ = 3982]. Furthermore, the 3474 Da peak was considerably larger than the 3983 Da peak, suggesting that with Aβ(1−42) monomers TGase primarily links Gln_{15} to Lys_{28} rather than Gln_{15} to Lys_{16}. Pepsin digestion following TGase cross-linking of Aβ-(1−42) fibrils also produced these cross-linked fragments, but with two notable differences (Figure 8D). First, the relative abundance of the 3474 Da fragment was much lower than that in the TGase-cross-linked monomer digest. This result is consistent with immunoblots like those in Figure 5. The lower immunostaining intensities of cross-linked dimer, trimer, and tetramer bands from Aβ aggregates relative to monomers were noted above, and less overall cross-linking would be expected to result in lower levels of cross-linked pepsin fragments. Second, the amount of the 3983 fragment relative to the 3474 fragment was much higher in pepsin digests of cross-linked fibrils. Analysis of MS ion currents from several digests indicated a 3983 to 3474 peak ratio of 0.29 ± 0.04 from Aβ monomers and of 1.8 ± 1.2 from fibrils. Current models of secondary structure in Aβ fibrils (*49*) place Gln_{15} near Lys_{16} at the end of intermolecular, parallel, in register β-strands formed by residues 18−26 (*50*), and this proximity may allow more efficient intermolecular

cross-linking of Gln_{15} in one Aβ peptide with Lys_{16} on an adjacent peptide compared to what can occur with monomers.

Although TGase cross-linking of monomers led to an increase in the level of β-structure based on the CD spectra in Figure 6A, the MS data suggest that most of this cross-linking involved linkage of Gln_{15} to Lys_{28} and thus would probably not be compatible with enhanced fibril formation. Previous reports are inconclusive. TGase treatment of Aβ(1−40) has been reported to induce formation of elongated structures that resemble protofibrils in EM images (*46*). However, TGase-catalyzed intramolecular cross-linking of tau, α-synuclein, and truncated Sup35 blocked both the nucleation and the fiber extension steps associated with amyloid fibril formation (*51*). It does not appear that any of the TGase cross-linking of monomeric Aβ(1−42) observed here involves intramolecular linkage of Gln_{15} to Lys_{28}. Such a cross-link would result in a loss of 17 Da (*52*) from $(M + H)^+$ of 4515 for Aβ(1−42), but only the 4515 peak was observed in mass spectra of TGase-cross-linked Aβ(1−42) prior to pepsin digestion (data not shown).

The immunostaining in Figure 5 suggested that glutaraldehyde or Cu(II) with peroxide is an effective cross-linker of both monomeric and aggregated Aβ(1−42). MALDI-TOF MS supports this conclusion, as peaks in the 4500−5000 mass range are largely eliminated in these cross-linked samples prior to pepsin digestion. However, few conclusions could be drawn about cross-linked Aβ residues from analysis of peptic fragments following treatment with these agents. With glutaraldehyde, cross-linking reactions must compete with piperidine formation resulting from cyclization at a single primary amine group (*53*). This reaction increases the mass of a peptide by 68 Da for each piperidine addition. Piperidine formation was the most obvious feature when peptic fragments of Aβ species cross-linked by glutaraldehyde were examined by MS. The peptic digest of cross-linked fibrils in Figure 8E gave prominent peaks at 2384 and 2452 Da, increments of 68 Da and twice 68 Da from the 2316 fragment corresponding to Aβ(1−19). This fragment contains two primary amine groups, the N-terminus and Lys_{16}, and both amines appear to be accessible to glutaraldehyde reaction in the fibrils. Less explicable in Figure 8E was the nearly complete loss of peaks corresponding to Aβ(4−19) (2000 Da) or Aβ(20−34) (1492 Da) in either piperidine-modified or unmodified form. A similar loss of the Aβ(4−19) peak was observed following pepsin digestion of glutaraldehyde-treated Aβ(1−42) monomer, although these digests contained some Aβ(20−34) and its piperidine adduct (data not shown). No peptic fragments with cross-links were detected following glutaraldehyde treatment. MS analysis of peptic fragments following cross-linking with Cu(II) and peroxide was not very informative. Sharp peaks corresponding to Aβ(1−19) (2315 Da) and Aβ(4−19) (2000 Da) were replaced by broad peaks, indicating that several oxidation products of varying mass had been generated on residue(s) in Aβ(1−19) (Figure 8F). These oxidative reactions did not appear to extend to Aβ(20−34), however, as a sharp peak at 1492 Da remained evident.

CONCLUSIONS

Other laboratories have reported the resolution of endogenous Aβ oligomers ranging in size from dimers to dodecamers by SEC and contended that some of these oligomers are primary toxic species in AD. In an effort to reconstitute soluble Aβ aggregates in vitro that resemble the endogenous soluble Aβ oligomers, we have generated soluble oligomers by incubation of synthetic Aβ(1−42) monomers in dilute SDS followed by dialysis. SEC and multiangle light scattering indicated a molecular mass of 150 kDa for the isolated oligomers (Figure 2A), but these oligomers partially dissociated in 1% LDS to give ∼40 kDa, 2−4mer, and monomer bands on SDS−PAGE (Figure 2B). Although the masses of these bands correspond to some of those reported for endogenous Aβ oligomers, the bands did not fractionate on SEC as a ladder of discrete species as reported for the endogenous oligomers. No SEC separation of discrete ∼40 kDa bands from apparent dimers and trimers in the 2−4mer bands was obtained in Figure 2B. Furthermore, these synthetic ∼40 kDa and 2−4mer bands were completely disaggregated to monomers by being boiled in 1% SDS (Figure 1B and ref *14*), in contrast to endogenous oligomer samples, which appear to be routinely boiled in sample buffer containing 1−2% SDS in preparation for SDS−PAGE without disruption of the oligomer gel bands (*10*, *11*). It appears that endogenous oligomeric Aβ aggregates are stabilized by an undefined process that has not yet been incorporated into in vitro Aβ aggregation procedures.

One hypothesis to define this process is that endogenous Aβ oligomers are stabilized by covalent cross-linking induced by unknown cellular agents. To develop techniques to examine this possibility, we have cross-linked synthetic Aβ(1−42) monomers and aggregates with three well-defined cross-linking agents and initiated the investigation of sensitive MS analyses to detect and characterize Aβ cross-linking. We first compared the efficiency of covalent cross-linking with these agents. Aβ monomers were cross-linked by TGase more efficiently than any of the three Aβ aggregates examined here (Figure 5G). Aggregation had a weaker effect on cross-linking by glutaraldehyde or Cu(II) with peroxide. The dependence of monomer loss on the concentration of these cross-linkers was similar for all four Aβ species (Figure 5H,I). We then assessed the effect of cross-linking on peptide secondary structure and thermal stability. Treatment of all four Aβ species with the three cross-linking agents in general had little effect on Aβ secondary structure as measured by CD. The one exception involved TGase cross-linking of Aβ monomers, where a modest increase in the level of β-structure was observed (Figure 7). However, the predominant β-structure in fibrils was stabilized by all three cross-linking agents, as indicated by retention of some β-structure in 1% SDS at high temperatures (Figure 6). In contrast, the β-structure in 2−4mers and oligomers was not stabilized following treatment with TGase or Cu(II) with peroxide and only partly stabilized by treatment with glutaraldehyde (Figure 6).

From the perspective of developing MS analyses to detect Aβ cross-linking and identify the cross-linked residues, our initial results here showed TGase to be the most useful cross-linking agent. Peptic fragments corresponding to each of the two possible sites of Aβ cross-linking by TGase were identified by MALDI-TOF MS (Figure 8C,D). Analysis of glutaraldehyde cross-linking was complicated by a competing side reaction in which piperidine was formed on single primary amine groups. Treatment with Cu(II) with peroxide led to very broad peaks in regions corresponding to peptic fragments Aβ(1−19) and Aβ(4−19), indicating formation of heterogeneous oxidation products that prevented precise interpretation of the reaction. These observations demonstrated that the convenience and speed of the MALDI-TOF technique allows a quick survey of a wide range of cross-linked samples and proteolysis conditions. However, additional peaks corresponding to larger cross-linked fragments were difficult to detect with this technique. Further analysis by

ESI-MS may reveal larger cross-linked species in a mass range where MALDI-TOF MS has low sensitivity.

In summary, these studies have characterized various synthetic Aβ(1−42) aggregates in terms of their size, thermal stability, susceptibility to cross-linking, thermal stability as a result of cross-linking, and sites of cross-linking. Endogenous Aβ aggregates have been difficult to isolate in quantities sufficiently large for characterization by these biochemical and biophysical techniques, and we anticipate that these studies with synthetic aggregates will add to current structural information that can be used for the rational design of agents for the treatment of AD.

ACKNOWLEDGMENT

We express our gratitude to Patricia Martin for technical assistance during the later stages of this investigation.

REFERENCES

1. Hardy, J., and Selkoe, D. J. (2002) The amyloid hypothesis of Alzheimer's disease: Progress and problems on the road to therapeutics. *Science 297*, 353–356.
2. Hartley, D. M., Walsh, D. M., Ye, C. P., Diehl, T., Vasquez, S., Vassilev, P. M., Teplow, D. B., and Selkoe, D. J. (1999) Protofibrillar intermediates of amyloid β-protein induce acute electrophysiological changes and progressive neurotoxicity in cortical neurons. *J. Neurosci. 19*, 8876–8884.
3. Klein, W. L., Krafft, G. A., and Finch, C. E. (2001) Targeting small Aβ oligomers: The solution to an Alzheimer's disease conundrum? *Trends Neurosci. 24*, 219–224.
4. Westerman, M. A., Cooper-Blacketer, D., Mariash, A., Kotilinek, L., Kawarabayashi, T., Younkin, L. H., Carlson, G. A., Younkin, S. G., and Ashe, K. H. (2002) The relationship between Aβ and memory in the Tg2576 mouse model of Alzheimer's disease. *J. Neurosci. 22*, 1858–1867.
5. Kawarabayashi, T., Shoji, M., Younkin, L. H., Lin, W. L., Dickson, D. W., Murakami, T., Matsubara, E., Abe, K., Ashe, K. H., and Younkin, S. G. (2004) Dimeric amyloid β protein rapidly accumulates in lipid rafts followed by apolipoprotein E and phosphorylated tau accumulation in the Tg2576 mouse model of Alzheimer's disease. *J. Neurosci. 24*, 3801–3809.
6. Lambert, M. P., Barlow, A. K., Chromy, B. A., Edwards, C., Freed, R., Liosatos, M., Morgan, T. E., Rozovsky, I., Trommer, B., Viola, K. L., Wals, P., Zhang, C., Finch, C. E., Drafft, G. A., and Klein, W. L. (1998) Diffusible, nonfibrillar ligands derived from Aβ_{1-42} are potent central nervous system neurotoxins. *Proc. Natl. Acad. Sci. U.S.A. 95*, 6448–6453.
7. Walsh, D. M., Klyubin, I., Fadeeva, J. V., Rowan, M. J., and Selkoe, D. J. (2002) Amyloid-β oligomers: Their production, toxicity and therapeutic inhibition. *Biochem. Soc. Trans. 30*, 552–557.
8. Hsia, A., Masliah, E., McConlogue, L., Yu, G., Tatsuno, G., Hu, K., Kholodenko, D., Malenka, R. C., Nicoll, R. A., and Mucke, L. (1999) Plaque-independent disruption of neural circuits in Alzheimer's disease mouse models. *Proc. Natl. Acad. Sci. U.S.A. 96*, 3228–3233.
9. Shankar, G. M., Li, S., Mehta, T. H., Garcia-Munoz, A., Shepardson, N. E., Smith, I., Brett, F. M., Farrell, M. A., Rowan, M. J., Lemere, C. A., Regan, C. M., Walsh, D. M., Sabatini, B. L., and Selkoe, D. J. (2008) Amyloid-β protein dimers isolated directly from Alzheimer's brains impair synaptic plasticity and memory. *Nat. Med. 14*, 837–842.
10. Lesne, S., Koh, M. T., Kotilinek, L., Kayed, R., Glabe, C. G., Yang, A., Gallagher, M., and Ashe, K. H. (2006) A specific amyloid-β protein assembly in the brain impairs memory. *Nature 440*, 352–357.
11. Townsend, M., Shankar, G. M., Mehta, T., Walsh, D. M., and Selkoe, D. J. (2006) Effects of secreted oligomers of amyloid β-protein on hippocampal synaptic plasticity: A potent role for trimers. *J. Physiol. 572*, 477–492.
12. Nichols, M. R., Moss, M. A., Reed, D. K., Lin, W.-L., Mukhopadhyay, R., Hoh, J. H., and Rosenberry, T. L. (2002) Growth of β-amyloid(1−40) protofibrils by monomer elongation and lateral association. Characterization of distinct products by light scattering and atomic force microscopy. *Biochemistry 41*, 6115–6127.
13. Rangachari, V., Reed, D. K., Moore, B. D., and Rosenberry, T. L. (2006) Secondary structure and interfacial aggregation of amyloid-β(1−40) on sodium dodecylsulfate micelles. *Biochemistry 45*, 8639–8648.
14. Rangachari, V., Moore, B. D., Reed, D. K., Sonoda, L. K., Bridges, A. W., Conboy, E., Hartigan, D., and Rosenberry, T. L. (2007) Amyloid-β(1−42) rapidly forms protofibrils and oligomers by distinct pathways in low concentrations of sodium dodecylsulfate. *Biochemistry 46*, 12451–12462.
15. Choo-Smith, L. P., Garzon-Rodriguez, W., Glabe, C. G., and Surewicz, W. K. (1997) Acceleration of amyloid fibril formation by specific binding of Aβ-(1−40) peptide to ganglioside-containing membrane vesicles. *J. Biol. Chem. 272*, 22987–22990.
16. Choo-Smith, L. P., and Surewicz, W. K. (1997) The interaction between Alzheimer amyloid β(1−40) peptide and ganglioside GM1-containing membranes. *FEBS Lett. 402*, 95–98.
17. Kakio, A., Nishimoto, S., Yanagisawa, K., Kozutsumi, Y., and Matsuzaki, K. (2002) Interactions of amyloid β-protein with various gangliosides in raft-like membranes: Importance of GM1 ganglioside-bound form as an endogenous seed for Alzheimer amyloid. *Biochemistry 41*, 7385–7390.
18. Yamamoto, N., Hirabayashi, Y., Amari, M., Yamaguchi, H., Romanov, G., Van Nostrand, W. E., and Yanagisawa, K. (2005) Assembly of hereditary amyloid β-protein variants in the presence of favorable gangliosides. *FEBS Lett. 579*, 2185–2190.
19. Nichols, M. R., Moss, M. A., Reed, D. K., Cratic-McDaniel, S., Hoh, J. H., and Rosenberry, T. L. (2005) Amyloid-β protofibrils differ from amyloid-β aggregates induced in dilute hexafluoroisopropanol in stability and morphology. *J. Biol. Chem. 280*, 2471–2480.
20. Nichols, M. R., Moss, M. A., Reed, D. K., Hoh, J. H., and Rosenberry, T. L. (2005) Rapid assembly of amyloid-β peptide at a liquid/liquid interface produces unstable β-sheet fibers. *Biochemistry 44*, 165–173.
21. Barghorn, S., Nimmrich, V., Striebinger, A., Krantz, C., Keller, P., Janson, B., Bahr, M., Schmidt, M., Bitner, R. S., Harlan, J., Barlow, E., Ebert, U., and Hillen, H. (2005) Globular amyloid β-peptide-(1−42) oligomer: A homogenous and stable neuropathological protein in Alzheimer's disease. *J. Neurochem. 95*, 834–847.
22. Kuo, Y. M., Webster, S., Emmerling, M. R., De Lima, N., and Roher, A. E. (1998) Irreversible dimerization/tetramerization and post-translational modifications inhibit proteolytic degradation of Aβ peptides of Alzheimer's disease. *Biochim. Biophys. Acta 1406*, 291–298.
23. Kalback, W., Watson, M. D., Kokjohn, T. A., Kuo, Y. M., Weiss, N., Luehrs, D. C., Lopez, J., Brune, D., Sisodia, S. S., Staufenbiel, M., Emmerling, M., and Roher, A. E. (2002) APP transgenic mice Tg2576 accumulate Aβ peptides that are distinct from the chemically modified and insoluble peptides deposited in Alzheimer's disease senile plaques. *Biochemistry 41*, 922–928.
24. Atwood, C. S., Scarpa, R. C., Huang, X., Moir, R. D., Jones, W. D., Fairlie, D. P., Tanzi, R. E., and Bush, A. I. (2000) Characterization of copper interactions with Alzheimer amyloid β peptides: Identification of an attomolar-affinity copper binding site on amyloid β1−42. *J. Neurochem. 75*, 1219–1233.
25. Atwood, C. S., Perry, G., Zeng, H., Kato, Y., Jones, W. D., Ling, K. Q., Huang, X., Moir, R. D., Wang, D., Sayre, L. M., Smith, M. A., Chen, S. G., and Bush, A. I. (2004) Copper mediates dityrosine cross-linking of Alzheimer's amyloid-β. *Biochemistry 43*, 560–568.
26. Dudek, S. M., and Johnson, G. V. (1994) Transglutaminase facilitates the formation of polymers of the β-amyloid peptide. *Brain Res. 651*, 129–133.
27. Benzinger, T. L. S., Gregory, D. M., Burkoth, T. S., Miller-Auer, H., Lynn, D. G., Botto, R. E., and Meredith, S. C. (1998) Propagating structure of Alzheimer's β-amyloid$_{(10-35)}$ is parallel β-sheet with residues in exact register. *Proc. Natl. Acad. Sci. U.S.A. 95*, 13407–13412.
28. Boutaud, O., Montine, T. J., Chang, L., Klein, W. L., and Oates, J. A. (2006) PGH2-derived levuglandin adducts increase the neurotoxicity of amyloid β1−42. *J. Neurochem. 96*, 917–923.
29. Boutaud, O., Ou, J. J., Chaurand, P., Caprioli, R. M., Montine, T. J., and Oates, J. A. (2002) Prostaglandin H2 (PGH2) accelerates formation of amyloid β1−42 oligomers. *J. Neurochem. 82*, 1003–1006.
30. Siegel, S. J., Bieschke, J., Powers, E. T., and Kelly, J. W. (2007) The oxidative stress metabolite 4-hydroxynonenal promotes Alzheimer protofibril formation. *Biochemistry 46*, 1503–1510.
31. Wilhelmus, M. M., Grunberg, S. C., Bol, J. G., van Dam, A. M., Hoozemans, J. J., Rozemuller, A. J., and Drukarch, B. (2009) Transglutaminases and transglutaminase-catalyzed cross-links colocalize with the pathological lesions in Alzheimer's disease brain. *Brain Pathol. 19*, 612–622.
32. Levine, H.III (1995) Soluble multimeric Alzheimer β(1−40) pre-amyloid complexes in dilute solution. *Neurobiol. Aging 16*, 755–764.
33. Fezoui, Y., Hartley, D. M., Harper, J. D., Khurana, R., Walsh, D. M., Condron, M. M., Selkoe, D. J., Lansbury, P. T. Jr., Fink, A. L., and

Teplow, D. B. (2000) An improved method of preparing the amyloid β-protein for fibrillogenesis and neurotoxicity experiments. *Amyloid 7*, 166–178.
34. LeVine, H. (1993) Thioflavine T interaction with synthetic Alzheimer's disease β-amyloid peptides: Detection of amyloid aggregation in solution. *Protein Sci. 2*, 404–410.
35. Debye, P. (1947) Molecular-weight determination by light scattering. *J. Phys. Colloid Chem. 51*, 18–32.
36. Zimm, B. H. (1948) The scattering of light and the radial distribution function of high polymer solutions. *J. Chem. Phys. 16*, 1093–1099.
37. Rizzi, C., Rossini, K., Bruson, A., Sandri, M., Dal Belin Peruffo, A., and Carraro, U. (2002) Fully reversible procedure for silver staining improves densitometry of complex mixtures of biopolymers resolved by sodium dodecyl sulfate-polyacrylamide gel electrophoresis. *Electrophoresis 23*, 3266–3269.
38. Kukar, T., Murphy, M. P., Eriksen, J. L., Sagi, S. A., Weggen, S., Smith, T. E., Ladd, T., Khan, M. A., Kache, R., Beard, J., Dodson, M., Merit, S., Ozols, V. V., Anastasiadis, P. Z., Das, P., Fauq, A., Koo, E. H., and Golde, T. E. (2005) Diverse compounds mimic Alzheimer disease-causing mutations by augmenting Aβ42 production. *Nat. Med. 11*, 545–550.
39. Tanaka, M., Chien, P., Yonekura, K., and Weissman, J. S. (2005) Mechanism of cross-species prion transmission: An infectious conformation compatible with two highly divergent yeast prion proteins. *Cell 121*, 49–62.
40. Walsh, D. M., Lomakin, A., Benedek, G. B., Condron, M. M., and Teplow, D. B. (1997) Amyloid β-protein fibrillogenesis: Detection of a protofibrillar intermediate. *J. Biol. Chem. 272*, 22364–22372.
41. Harper, J. D., Wong, S. S., Lieber, C. M., and Lansbury, P. T. Jr. (1997) Observation of metastable Aβ amyloid protofibrils by atomic force microscopy. *Chem. Biol. 4*, 119–125.
42. Goldsbury, C. S., Wirtz, S., Muller, S. A., Sunderji, S., Wicki, P., Aebi, U., and Frey, P. (2000) Studies on the *in vitro* assembly of Aβ 1−40: Implications for the search for Aβ fibril formation inhibitors. *J. Struct. Biol. 130*, 217–231.
43. Hepler, R. W., Grimm, K. M., Nahas, D. D., Breese, R., Dodson, E. C., Acton, P., Keller, P. M., Yeager, M., Wang, H., Shughrue, P., Kinney, G., and Joyce, J. G. (2006) Solution state characterization of amyloid β-derived diffusible ligands. *Biochemistry 45*, 15157–15167.
44. Yu, L., Edalji, R., Harlan, J. E., Holzman, T. F., Lopez, A., Labkovsky, B., Hillen, H., Barghorn, S., Ebert, U., Richardson, P. L., Miesbauer, L., Solomon, L., Bartley, D., Walter, K., Johnson, R. W., Hajduk, P. J., and Olejniczak, E. T. (2009) Structural characterization of a soluble amyloid β-peptide oligomer. *Biochemistry 48*, 1870–1877.
45. Reynolds, J. A., and Tanford, C. (1970) Binding of dodecyl sulfate to proteins at high binding ratios. Possible implications for the state of proteins in biological membranes. *Proc. Natl. Acad. Sci. U.S.A. 66*, 1002–1007.
46. Hartley, D. M., Zhao, C., Speier, A. C., Woodard, G. A., Li, S., Li, Z., and Walz, T. (2008) Transglutaminase induces protofibril-like amyloid β-protein assemblies that are protease-resistant and inhibit long-term potentiation. *J. Biol. Chem. 283*, 16790–16800.
47. Kheterpal, I., Williams, A., Murphy, C., Bledsoe, B., and Wetzel, R. (2001) Structural features of the Aβ amyloid fibril elucidated by limited proteolysis. *Biochemistry 40*, 11757–11767.
48. Chen, M., Cook, K. D., Kheterpal, I., and Wetzel, R. (2007) A triaxial probe for on-line proteolysis coupled with hydrogen/deuterium exchange-electrospray mass spectrometry. *J. Am. Soc. Mass Spectrom. 18*, 208–217.
49. Tycko, R. (2004) Progress towards a molecular-level structural understanding of amyloid fibrils. *Curr. Opin. Struct. Biol. 14*, 96–103.
50. Lührs, T., Ritter, C., Adrian, M., Riek-Loher, D., Bohrmann, B., Döbeli, H., Schubert, D., and Riek, R. (2005) 3D structure of Alzheimer's amyloid-β(1−42) fibrils. *Proc. Natl. Acad. Sci. U.S.A. 102*, 17342–17347.
51. Konno, T., Morii, T., Hirata, A., Sato, S., Oiki, S., and Ikura, K. (2005) Covalent blocking of fibril formation and aggregation of intracellular amyloidgenic proteins by transglutaminase-catalyzed intramolecular cross-linking. *Biochemistry 44*, 2072–2079.
52. Schmid, A. W., Chiappe, D., Pignat, V., Grimminger, V., Hang, I., Moniatte, M., and Lashuel, H. A. (2009) Dissecting the mechanisms of tissue transglutaminase-induced cross-linking of α-synuclein: Implications for the pathogenesis of Parkinson disease. *J. Biol. Chem. 284*, 13128–13142.
53. Russo, A., Chandramouli, N., Zhang, L., and Deng, H. (2008) Reductive glutaraldehydation of amine groups for identification of protein N-termini. *J. Proteome Res. 7*, 4178–4182.